

Supporting Information

Realizing Solution-Processed Monolithic PbS QDs/ Perovskite Tandem Solar Cells with High UV Stability

Yannan Zhang,^a Mengfan Gu,^a Ning Li,^b Yalong Xu,^a Xufeng Ling,^a Yongjie Wang,^a Sijie Zhou,^a Fangchao Li,^a Fan Yang,^a Kang Ji,^a Jianyu Yuan,^{a,*} and Wanli Ma^{a,*}

^aInstitute of Functional Nano & Soft Materials (FUNSOM), Jiangsu Key Laboratory for Carbon-Based Functional Materials & Devices, Joint International Research Laboratory of Carbon-Based Functional Materials and Devices, Soochow University
199 Ren-Ai Road, Suzhou Industrial Park, Suzhou, Jiangsu 215123, P. R. China
E-mail: jyyuan@suda.edu.cn (J. Y.), wlma@suda.edu.cn (W. M.)

^bInstitute of Materials for Electronics and Energy Technology (i-MEET)
Friedrich-Alexander-University Erlangen-Nuremberg Martensstraße 7, 91058 Erlangen, Germany

Content

1. Materials synthesis
2. Devices fabrications and characterizations
3. Solar cell performances
4. UV-*vis* absorption
5. External quantum efficiency
6. UPS spectra
7. Atomic Force Microscopy

Materials: Lead acetate trihydrate (99.9%, Alfa), 1-octadecene (ODE) (tech. grade, 90%, J&K), oleic acid (OA) (tech. grade, 90%, Alfa), bis(trimethylsilyl) sulfide $[(\text{TMS})_2\text{S}]$ (98%, J&K), hexane (95%, J&K), acetone (99.5%, J&K), isopropanol (95%, J&K), tetra-n-butylammonium iodide (TBAI) (98%, Alfa), 1,2-ethanedithiol (EDT) (98.0%, Sigma-Aldrich), acetonitrile (99%, Alfa), methanol (99%, Fluka), *n*-PEDOT (high-conductivity grade, Sigma-Aldrich), SnO₂ nanoparticles (Alfa Aesar, 15% in water), PbI₂ (99.999%, beads; Alfa Aesar), MAI (99.5%; Xi'an Polymer Light Technology Corp.), spiro-OMeTED (99.5%; Xi'an Polymer Light Technology Corp.), dimethylacetamide (99%; Sigma-Aldrich), N-Methyl-2-pyrrolidone (99.5%, J&K), chlorobenzene (99.8%; Sigma-Aldrich).

Synthesis of Colloidal Quantum Dots: The QDs used during fabrication were synthesized and purified according to a previously reported method.^[1] Briefly, 10mmol of lead acetate trihydrate and 7 g of oleic acid (OA) were dissolved in 60 g of 1-octadecene (ODE) in a three-neck flask by heating the mixture to 100 °C under vacuum for 2 h. The sulfide precursor was prepared separately by mixing 1 mL of hexamethyldisilathiane and 9 mL of 1-octadecene. The reaction was initiated by rapid injection of the sulfide precursor into the lead precursor solution. The QDs, with the excitonic absorption peaks at $\lambda=855$ nm, 1038 nm and 1254 nm were grown at the desired temperature for an optimal time (10 min, 1 min, 45 s for 75°C, 145°C, 180°C respectively). The as-synthesized solution was transferred into a nitrogen-filled glovebox. QDs were purified by adding a mixture of hexane and isopropanol and then redispersed in hexane and precipitated with acetone, followed by centrifugation. The extracted QDs were stored in the glovebox. For device fabrication, PbS QDs were redispersed in hexane.

Synthesis of ZnO Nanoparticles: ZnO nanoparticles were synthesized according to literature procedures.^[2] 2.95 g (13.4 mmol) Zinc acetate dehydrate was dissolved in 125 ml

methanol with stirring at 63.5 °C. A solution of KOH (1.48 g, 23 mmol) in 65 ml methanol was then dropwise added over a period of 15 min. The mixed solution was continuously stirred for 2.5 h. After cooling to room temperature, the solution was then centrifuged and washed with methanol for twice. Methanol (10 ml) and chloroform (10 ml) were added to disperse the precipitate. Before use, the ZnO nanoparticles solution were filtered through a 0.22 mm PVDF (polyvinylidene difluoride) syringe filter.

Fabrication of Single-Junction Solar Cells: Patterned ITO anodes were sequentially cleaned by deionized water, isopropanol, and acetone in an ultrasonic apparatus and then followed by 15 min of UV-ozone treatment. ZnO nanoparticles were deposited at 2500rpm for 15 s on ITO substrate. The PbS-QDs layers were fabricated through layer-by-layer deposition method. PbS-TBAI films were prepared by spinning coating PbS QDs from 10 mg/mL hexane solution at 2500 rpm. The post ligand exchange was carried out by soaking the as-prepared film in 10 mg/mL TBAI methanol solution for 30 s, and followed by two rinse-spin steps with acetonitrile. This procedure was repeated for several times to obtain desired thickness. After the deposition of PbS-TBAI layers, PbS-EDT layers were immediately deposited on top of PbS-TBAI layers. 10 mg/mL PbS was spin coated at 2500 rpm for 10 s. The resulting films were soaked in EDT (0.04 vol% in acetonitrile) for 30 s and washed with acetonitrile for twice. This procedure was repeated for twice. The prepared devices were stored in air and sequentially annealed at 60 °C for several hours. Finally, a 100 nm Au layer (0.5 Å/s) was evaporated through e-beam deposition method onto the PbS layers under high vacuum lower than 1×10^{-5} mbar and the active area of each device is 7.25 mm². For the rear single-junction reference cells, SnO₂ nanoparticles were diluted by H₂O and IPA with a ratio of 1:6.5:3.5. The final solution was spin coated onto ITO substrate at 3000 rpm for 30s. The MAPbI₃ precursor solution was prepared by an equimolar mixture of PbI₂ with MAI in dimethylacetamide: N-Methyl-2-

pyrrolidone (8:2, v/v) at 70 °C, and the total concentration is 1.0 M. The solution was coated onto the SnO₂ substrate and spun at 1000 and 5000 rpm for 10 and 40 s, respectively. After reaching high-speed rotation for about 10 s, 50 μL of toluene was promptly dripped onto the substrate. Then, a solution of 2,2',7,7'-tetrakis(N,N-dip-methoxyphenylamine)-9,9'-spirobifluorene (Spiro-OMeTAD, 90 mg) in anhydrous chlorobenzene (1 mL) was mixed with 22 μL of lithium bis-(trifluoromethanesulfonyl) imide solution (520 mg/mL in anhydrous acetonitrile) and 36 μL 4-tertbutylpyridine and spin-coated on the MAPbI₃ film at 5000 rpm for 30 s. Finally, silver (Ag) (100 nm) as the cathode was deposited on the MoO₃ (8 nm) in vacuum thermal evaporator.

Fabrication of Tandem Solar Cells: The fabrication of the front and rear cells according to the preparation of single-junction solar cells. For the fabrication of recombination layer, a modified n-PEDOT was deposited on top of PbS-EDT layers at 2000 rpm followed by annealing at 100 °C for 5 min. To prepare n-PEDOT, 1 mL n-PEDOT was diluted with 3 mL deionized water before the addition of 10 mg of surfactant (Capstone FS-31). SnO₂ nanoparticles were diluted by H₂O and IPA with a ratio of 1:6.5:3.5. The final solution was spin coated onto ITO substrate at 3000 rpm for 30s. The subsequent fabrication of rear subcells was the same with single-junction devices.

Fabrication of Perovskite Single-Junction Solar Cells: Patterned ITO anodes were sequentially cleaned by deionized water, isopropanol, and acetone in an ultrasonic apparatus and then followed by 15 min of UV-ozone treatment. SnO₂ nanoparticles were diluted by H₂O and isopropyl alcohol (IPA) with a ratio of 1:6.5:3.5. The final solution was spin coated onto ITO substrate at 3000 rpm for 30s.

a. One-step process with annealing treatment method: The MAPbI₃ precursor solution was prepared by an equimolar mixture of PbI₂ with MAI in anhydrous dimethyl sulfoxide: γ-

butyrolactone (3:7, v/v) at room temperature, and the total concentration is 1.2 M. The solution was coated onto the SnO₂ substrate and spun at 1000 and 4000 rpm for 10 and 40 s, respectively. During the high-speed spin-coating step, 150 μL of chlorobenzene was promptly dripped onto the substrate 14 s preliminary to the end of the process. The substrate was then dried at 100 °C for 10 min.

b. One-step process without annealing treatment method: The MAPbI₃ precursor solution was prepared by an equimolar mixture of PbI₂ with MAI in dimethylacetamide: N-Methyl-2-pyrrolidone (8:2, v/v) at 70 °C, and the total concentration is 1.0 M. The solution was coated onto the SnO₂ substrate and spun at 1000 and 5000 rpm for 10 and 40 s, respectively. After reaching high-speed rotation for about 10 s, 50 μL of toluene was promptly dripped onto the substrate.

c. Two-step process without annealing treatment method: 1.0 M of PbI₂ in dimethylformamide (DMF) was spin coated onto the electron transport layer at 3000 rpm for 30 s, after the solvent volatilized, the solution of MAI (10 mg in 1 ml IPA) was spin coated onto the PbI₂ at 4000 rpm for 20 s, and then the film was taken out from the glove box and stored in ambient air (10%–20% humidity) for 1 h. To prevent the residual solvent and thioalcohol ligand in the PbS front cell diffuse into the rear cell and cause detrimental effect on the perovskite layer when annealing, the two-step perovskite solar cells were fabricated without thermal annealing treatment.

Then, a solution of 2,2',7,7'-tetrakis(N,N-dip-methoxyphenylamine)-9,9'-spirobifluorene (Spiro-OMeTAD, 90 mg) in anhydrous chlorobenzene (1 mL) was mixed with 22 μL of lithium bis-(trifluoromethanesulfonyl) imide solution (520 mg/mL in anhydrous acetonitrile) and 36 μL 4-tertbutylpyridine and spin-coated on the MAPbI₃ film at 5000 rpm for 30 s. Finally, silver

(Ag) (100 nm) as the cathode was deposited on the MoO₃ (8 nm) in vacuum thermal evaporator. The area of each device is 7.25 mm² which was defined through a shadow mask.

Characterization of Solar Cell Devices: The performance of all cells were tested under AM 1.5G illumination (Newport, Class AAA solar simulator, 94023A-U). The EQE was determined using a certified IPCE equipment (Zolix Instruments, Inc, SolarCellScan100). UV–vis–NIR spectra were recorded on a Perkin Elmer model Lambda 750 and 950. AFM images were obtained with a Veeco Multimode V instrument. Device stability under UV illumination is carried out using a 325 nm ultraviolet lamp. Optical constants including real and imaginary refractive indexes (n, k) were measured by ellipsometry.

Optical simulations: The J_{sc} of bottom and top sub-cells is calculated as:

$$J_{sc,bottom}(E_{g,1}) = e \int_{E_{g,1}}^{\infty} I_{ph}(E) \times EQE_1(E) \times (1 - mirror_{loss}) \times dE \quad (1)$$

$$J_{sc,top}(E_{g,2}) = e \int_{E_{g,2}}^{\infty} I_{ph}(E) \times EQE_2(E) \times \left[1 - \frac{EQE_1(E)}{IQE_1(E)} (1 - mirror_{loss}) \right] \times dE \quad (2)$$

where $E_{g,1}$ is the bandgap energy of the PbS used in the bottom sub-cell (1.3 eV), $E_{g,2}$ the bandgap energy of the perovskite used in the top sub-cell (1.5 eV), I_{ph} the flux of photons in AM1.5G and EQE_1/ IQE_1 absorption of the bottom sub-cell. $Mirror_{loss}$ represents the loss of absorption in the cell implemented in the tandem versus the stand-alone single cell that would have a perfect mirror as a top electrode. This loss is induced by the absence of significant reflection at the interface between the bottom sub-cell and the intermediate layer.

Figure S1. *J-V* curves of optimal PbS QDs single-junction solar cells.

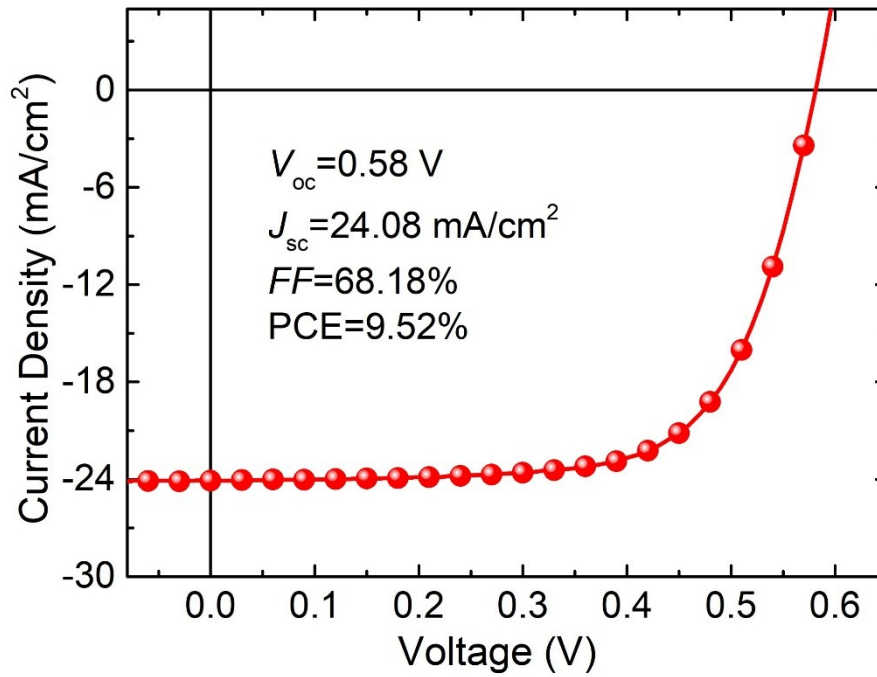


Figure S2. *J-V* curves of perovskite solar cells using one-step without annealing method with different substrate.

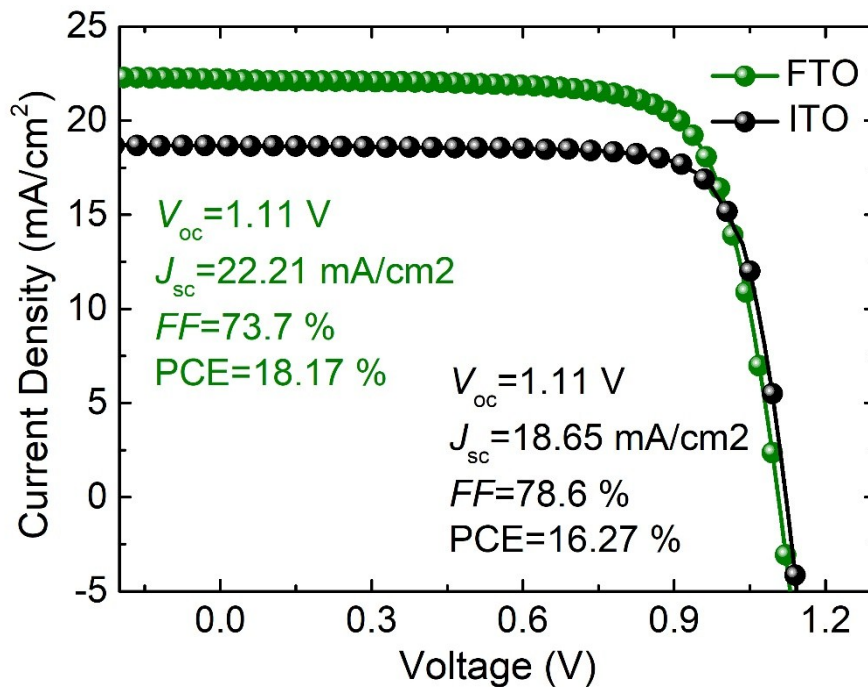


Figure S3. *J-V* curves of tandem solar cells with different perovskite deposition procedures.

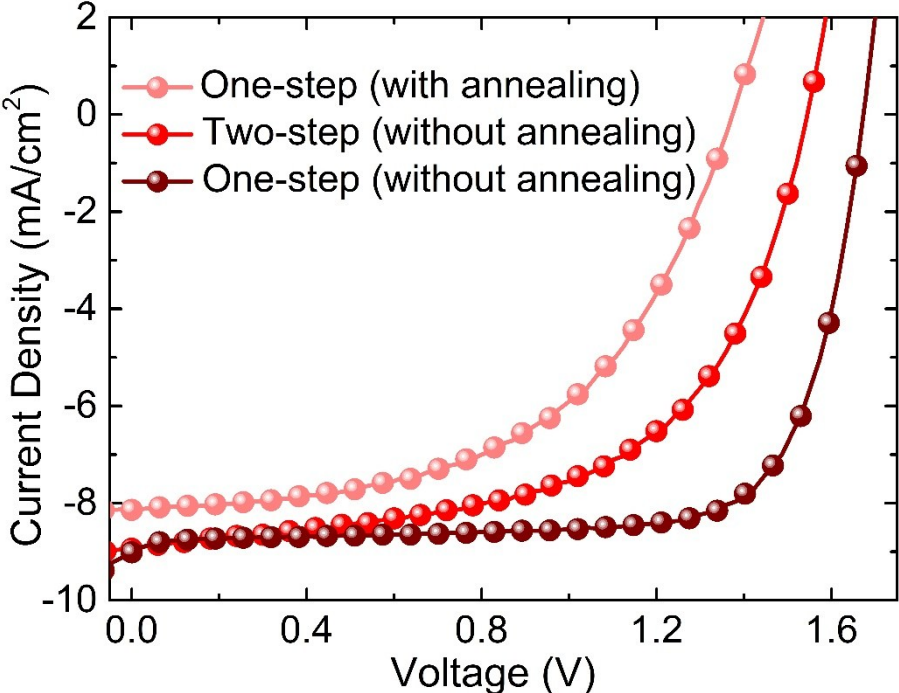


Figure S4. *J-V* curves of tandem solar cell with the highest V_{oc} .

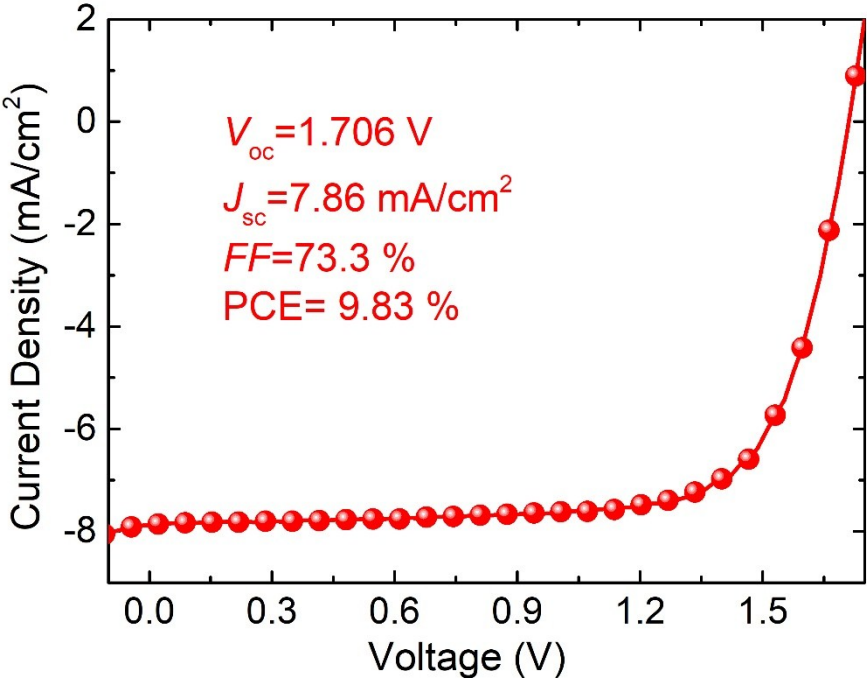


Figure S5. UPS spectra of a) *n*-PEDOT and b) SnO₂.

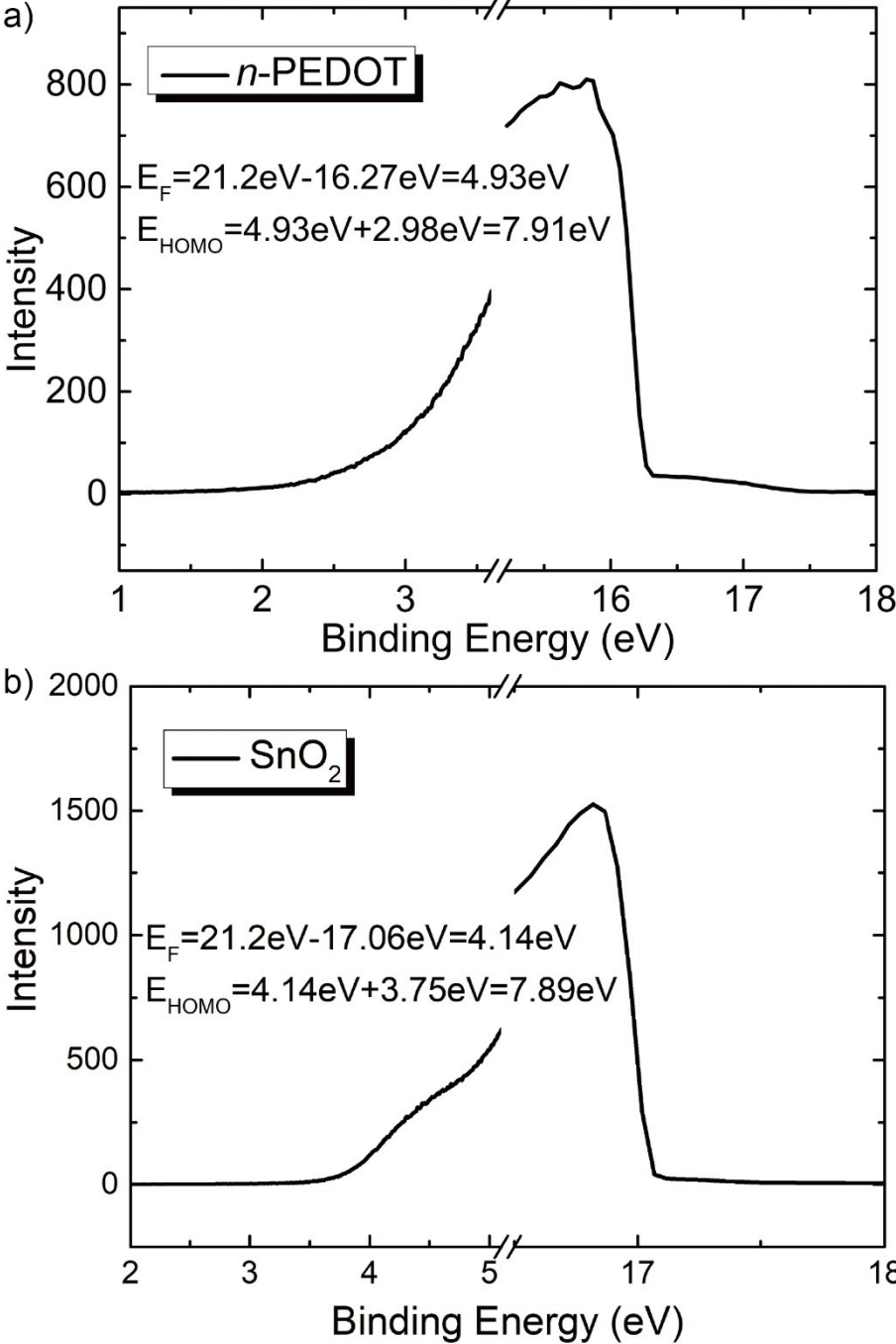


Figure S6. AFM height images for a) SnO₂ without IPA, b) with IPA and AFM phase images for c) SnO₂ without IPA, d) with IPA.

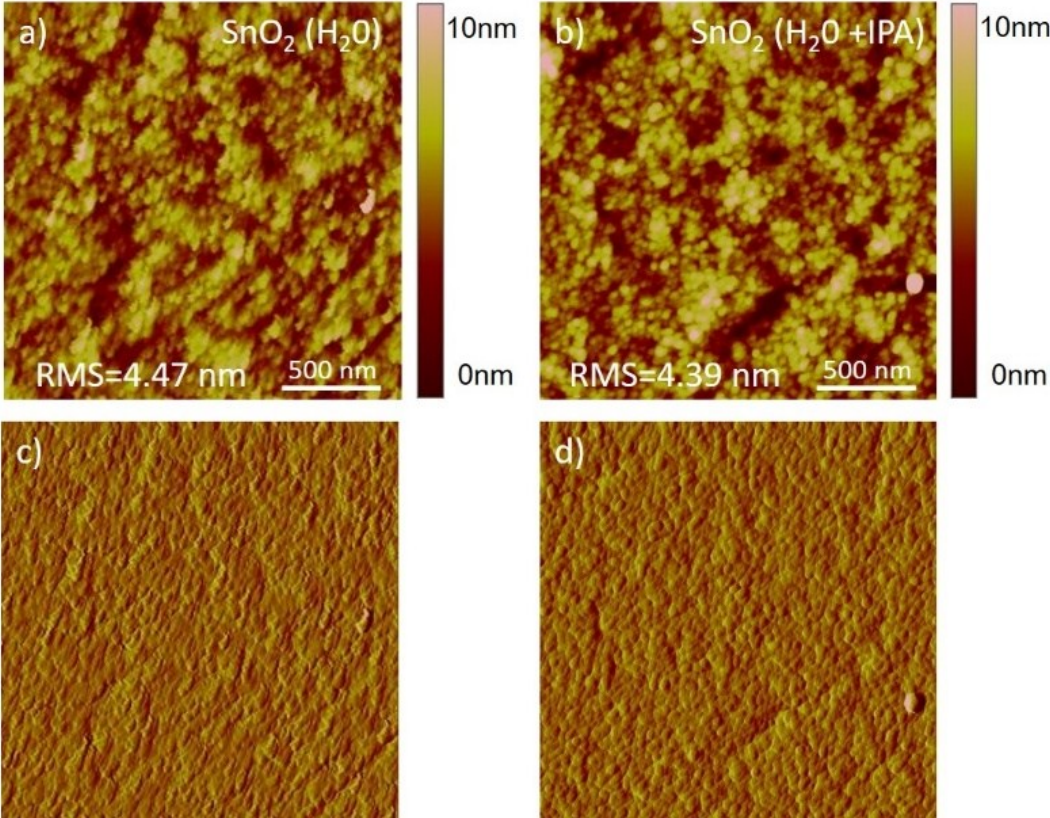


Figure S7. *J-V* curves of tandem solar cells using one-step method without annealing at different concentration of perovskite solution.

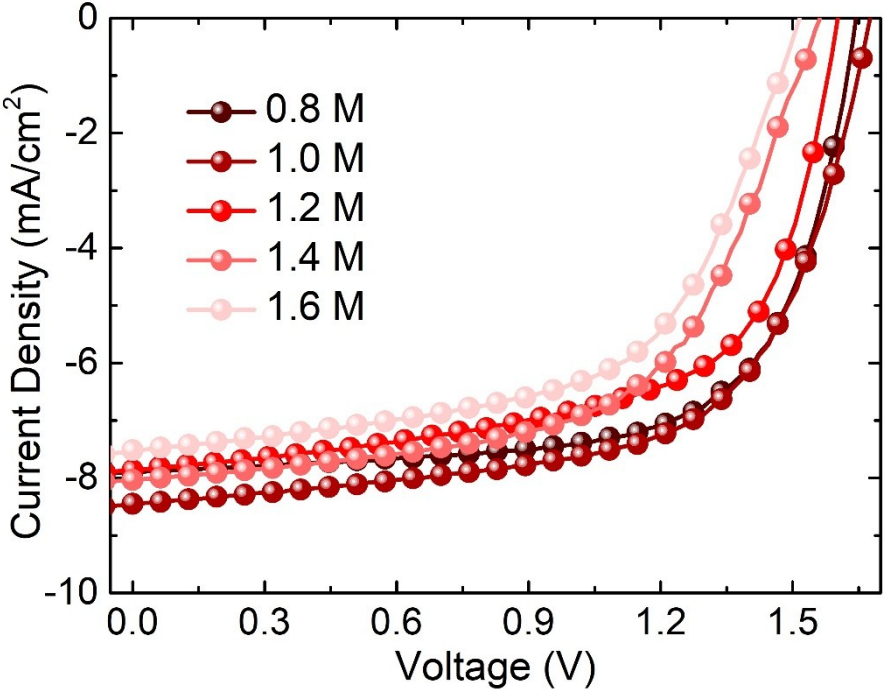


Figure S8. a) Solvent absorption of PbS QDs with different absorption peaks. b) Absorption of PbS and perovskite thin films.

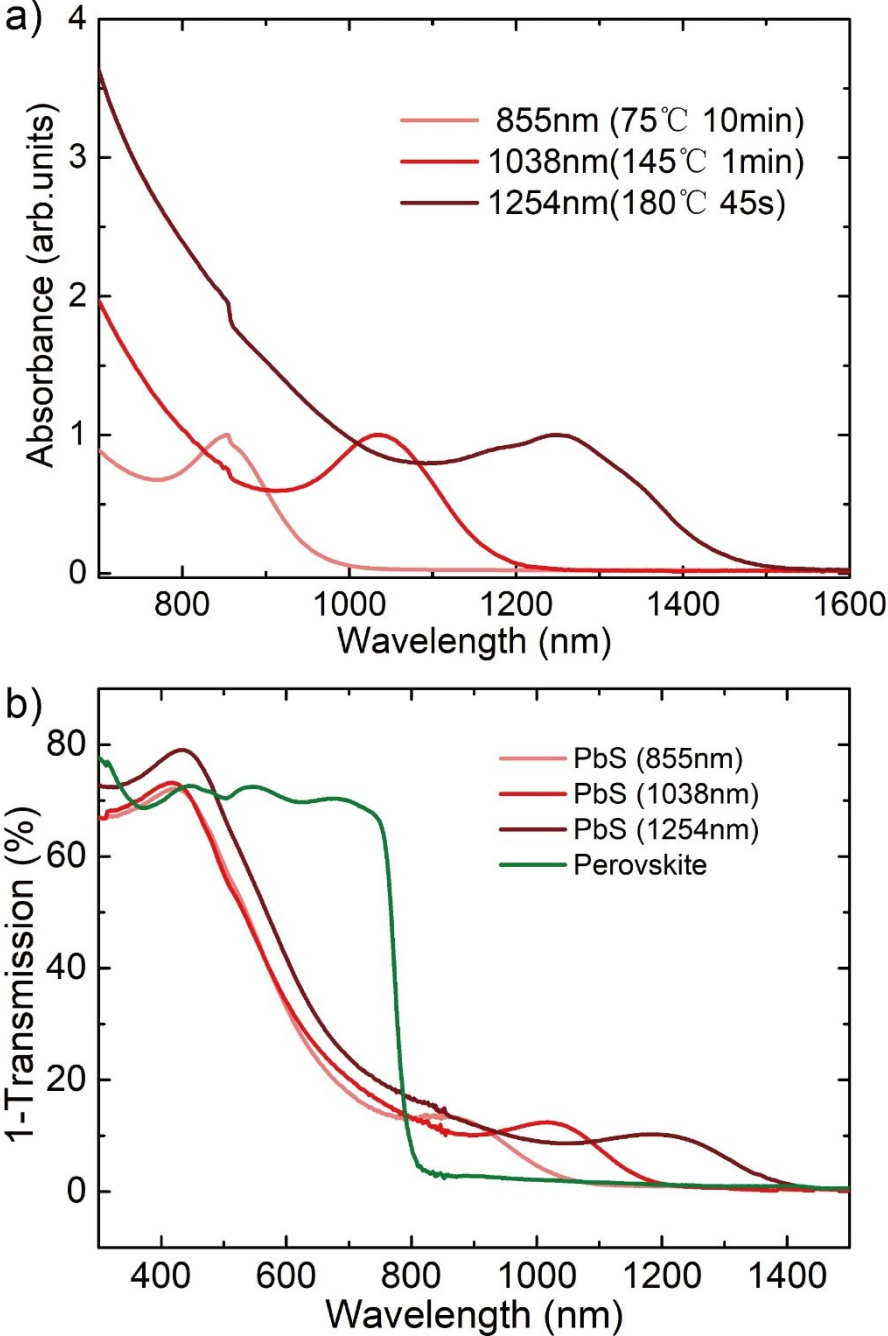


Figure S9. a) EQE spectrum of perovskite reference cells. b) EQE spectrum of PbS QDs reference cells with exciton peak at 1038 nm and 1254 nm.

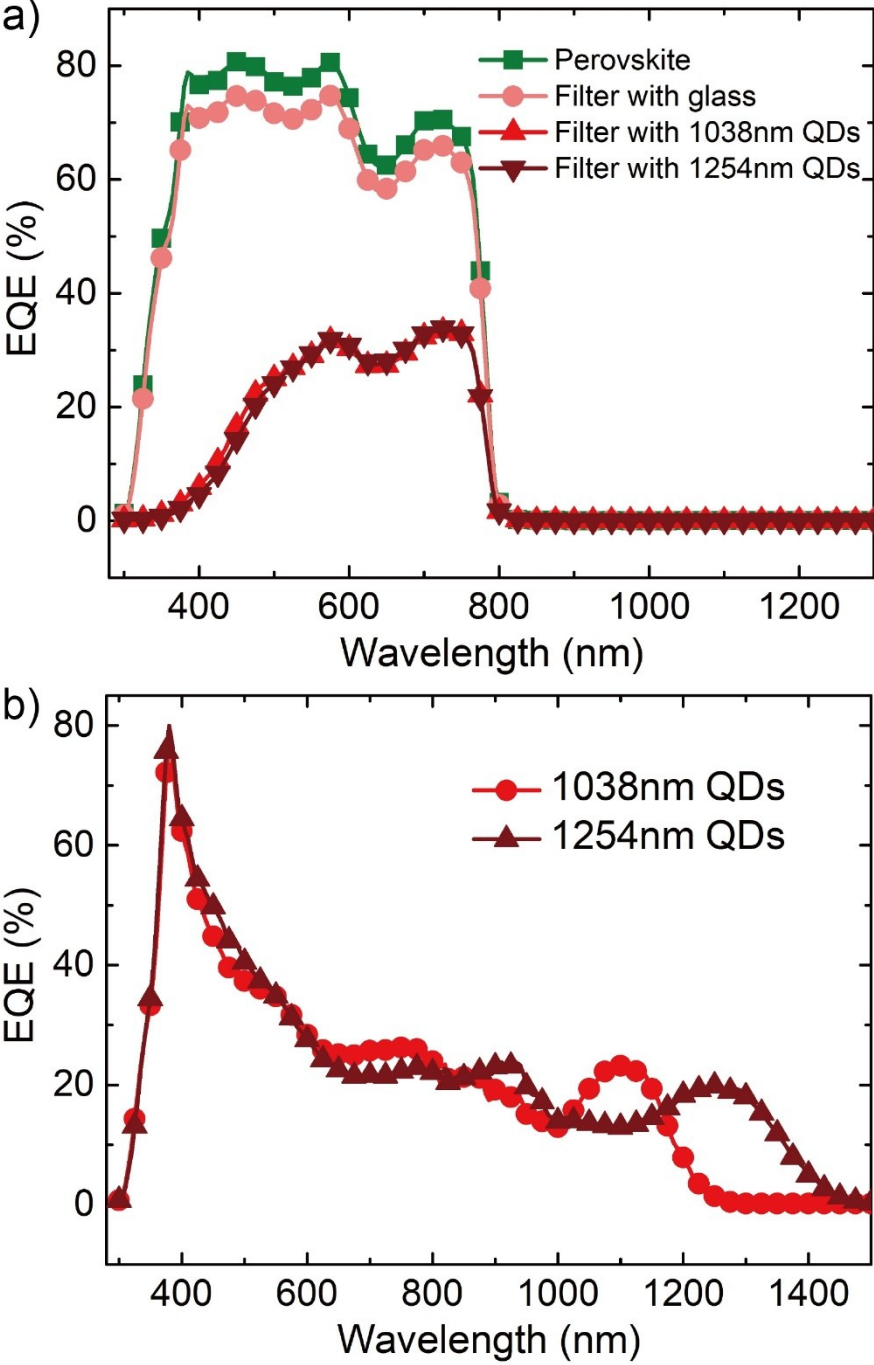


Figure S10. FF histogram distribution of sixty devices.

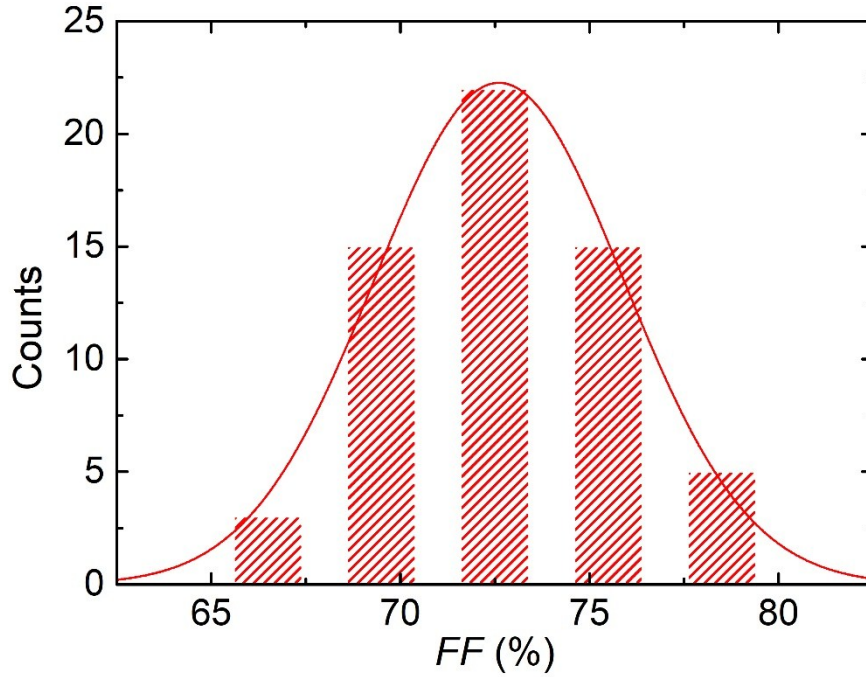


Figure S11. Thickness and optical constant (real and imaginary refractive index: n , k) of each layer in the PbS QDs/perovskite tandem solar cell used for the optical simulation.

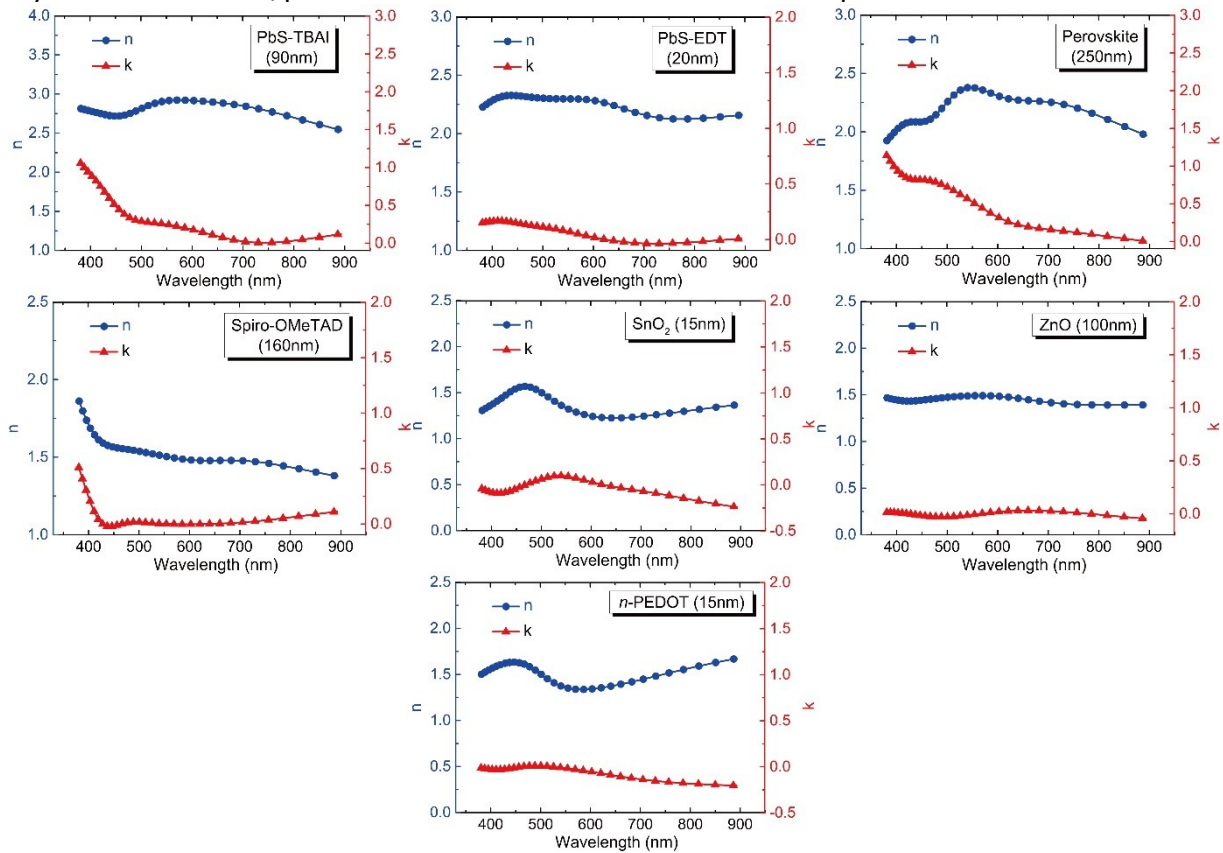


Table S1. Subcell device performance with different PbS QDs concentration for PbS-EDT layer with a structure of ITO/ ZnO/ PbS-TBAI/ PbS-EDT/ Au when the thickness of PbS-TBAI is kept at 75 nm.

PbS concentration (mg/ml)	Layer	V_{oc} (V)	J_{sc} (mA/cm ²)	FF (%)	PCE (%)
20	2	0.58	13.01	68.6	5.18
10	2	0.39	14.05	57.6	3.16
5	2	0.31	14.42	55.9	2.50
	1	0.22	15.32	52.7	4.78

Table S2. PbS QDs solar cell device performance with different annealing temperatures and time. The PbS concentration for PbS-EDT layer is 10 mg/ml.

Temperature (°C)	Time (h)	V_{oc} (V)	J_{sc} (mA/cm ²)	FF (%)	PCE (%)
40	2	0.53	13.65	69.2	5.01
	3	0.54	14.22	67.9	5.21
	4	0.55	14.34	68.3	5.39
	4.5	0.55	13.77	70.2	5.32
	5	0.55	14.58	70.1	5.62
	8	0.57	14.01	68.5	5.47
60	2	0.53	14.06	67.3	5.02
	3	0.55	14.27	67.5	5.30
	4	0.55	14.79	70.1	5.70
	4.5	0.54	14.28	68.8	5.31
	5	0.57	14.56	69.5	5.77
	8	0.57	13.81	68.7	5.41
80	0.5	0.47	14.72	64.9	4.49
	2	0.54	14.16	68.1	5.21
	3	0.55	13.07	67.6	4.86
	4	0.55	13.42	66.4	4.90
	4.5	0.56	13.65	67.9	5.19
	5	0.56	14.34	69.1	5.55
	8	0.57	12.93	68.2	5.03

Table S3. Device optimization of perovskite solar cells using room-temperature two-step solution processing techniques with a structure of ITO/ SnO₂/ PbI₂/ MAI/ Spiro-OMeTAD/ MoO₃/ Ag.

PbI ₂	MAI	Loading Time(s)	V _{oc} (V)	J _{sc} (mA/cm ²)	FF (%)	PCE (%)
420 mg/ml	10 mg/ml	20	1.01	19.09	61.8	11.92
		30	1.01	18.33	60.4	11.18
		40	1.02	18.66	63.3	12.05
		50	1.01	19.07	60.1	11.58
	40 mg/ml	20	0.98	18.90	66.1	12.24
		30	0.95	19.27	65.3	11.95
		40	0.90	19.77	64.8	11.53
		50	0.87	19.77	62.5	10.75
	70 mg/ml	20	0.86	19.61	61.9	10.44
		30	0.86	19.96	59.7	10.25
		40	0.83	19.46	61.5	9.93
		50	0.78	20.32	57.9	9.18
460 mg/ml	10 mg/ml	20	1.01	19.57	65.6	12.97
		30	1.01	19.65	62.1	12.32
		40	1.02	19.52	62.8	12.50
		50	1.02	19.97	60.9	12.40
	40 mg/ml	20	0.99	20.63	61.8	12.62
		30	0.95	19.68	61.0	11.40
		40	0.98	20.15	62.6	12.36
		50	0.96	20.14	61.6	11.91
	70 mg/ml	20	0.81	20.30	62.1	10.21
		30	0.78	19.77	60.2	9.28
		40	0.78	20.93	61.0	9.96
		50	0.74	20.01	60.5	8.96
500 mg/ml	10 mg/ml	20	1.04	19.44	66.5	13.44
		30	1.04	19.10	62.3	12.38
		40	1.04	19.63	64.0	13.07
		50	1.02	19.36	61.2	12.09
	40 mg/ml	20	1.01	20.11	70.7	14.36
		30	0.95	20.36	69.4	13.42
		40	0.99	20.55	60.4	12.29
		50	0.92	19.92	67.8	12.43
	70	20	0.90	20.38	70.7	12.97

mg/ml	30	0.90	20.08	68.2	12.33
	40	0.90	20.07	72.1	13.02
	50	0.81	19.78	60.7	9.73

Table S4. Tandem device performance with different kinds of PEDOT.

PEDOT	V_{oc} (V)	J_{sc} (mA/cm ²)	FF (%)	PCE (%)
PEDOT (AI 4083)	1.06	8.04	37.2	3.17
PEDOT (PH 1000)	1.26	8.88	53.1	5.94
<i>n</i> -PEDOT	1.50	9.30	52.3	7.30

Table S5. Tandem device performance with different ratios of *n*-PEDOT:H₂O.

<i>n</i> -PEDOT:H ₂ O	V_{oc} (V)	J_{sc} (mA/cm ²)	FF (%)	PCE (%)
1:1	1.53	8.55	48.7	6.37
1:1.5	1.53	8.16	53.7	6.70
1:2	1.57	8.61	61.8	8.35
1:3	1.57	8.75	65.0	8.93
1:4	1.55	7.60	60.1	7.08
1:5	1.53	7.73	59.7	7.06
1:6	1.40	6.88	58.1	5.60
1:7	1.40	7.72	58.7	6.34
1:8	1.36	7.27	58.3	5.76

Table S6. Tandem device performance with different annealing time of *n*-PEDOT.

Time (min)	V_{oc} (V)	J_{sc} (mA/cm ²)	FF (%)	PCE (%)
5	1.66	8.99	58.2	8.69
10	1.64	8.99	69.6	10.26
20	1.57	8.92	60.6	8.49
30	1.51	8.86	60.7	8.12

Table S7. Tandem device performance with different ratios of SnO₂:H₂O:IPA.

SnO ₂ :H ₂ O:IPA	V_{oc} (V)	J_{sc} (mA/cm ²)	FF (%)	PCE (%)
--	--------------	--------------------------------	--------	---------

1:6.5:0	1.40	8.29	60.5	7.02
1:6.5:1.5	1.55	8.58	63.3	8.42
1:6.5:2.5	1.53	8.40	66.3	8.52
1:6.5:3.5	1.62	8.44	68.3	9.34
1:6.5:4.5	1.51	8.73	65.3	8.61
1:10:0	1.36	8.60	54.1	6.33

Table S8. Tandem device performance with different recombination layers.

RL	V_{oc} (V)	J_{sc} (mA/cm ²)	FF (%)	PCE (%)
Au/ ZnO NPs	1.17	7.20	59.6	5.02
Au/ SnO ₂	1.40	8.37	60.8	7.12
Au/ Nb ₂ O ₅	1.30	4.97	55.4	3.58
Au/ <i>n</i> -PEDOT/ SnO ₂	1.62	7.87	66.9	8.53
<i>n</i> -PEDOT/ SnO ₂	1.68	7.78	70.3	9.19
<i>n</i> -PEDOT/ Au/ SnO ₂	1.64	7.83	65.8	8.45
<i>n</i> -PEDOT/ Nb ₂ O ₅	1.44	7.55	20.5	2.23
ITO(sputtered)/ Nb ₂ O ₅	1.12	10.91	56.6	6.92
ITO(sputtered)/ SnO ₂	1.36	10.77	61.7	9.04
MoO ₃ / Ag/ ZnO NPs	0.88	7.65	48.5	3.27
MoO ₃ / Ag/ SnO ₂	0.77	7.12	55.5	3.04

Table S9. Tandem device performance with different PbS-TBAI thickness.

Thickness (nm)	V_{oc} (V)	J_{sc} (mA/cm ²)	FF (%)	PCE (%)
150	1.57	6.68	79.1	8.30
135	1.57	7.77	76.7	9.36
120	1.62	7.54	75.5	9.22
105	1.62	7.79	74.2	9.36
90	1.62	8.38	74.0	10.05
75	1.62	8.45	71.0	9.72
60	1.57	8.29	73.1	9.51

Table S10. Tandem device performance with different perovskite concentrations (an equimolar mixture of PbI₂ with MAI in dimethylacetamide: N-Methyl-2-pyrrolidone (8:2, v/v)).

Concentration (mol)	V_{oc} (V)	J_{sc} (mA/cm ²)	FF (%)	PCE (%)
---------------------	--------------	--------------------------------	--------	---------

0.8	1.66	7.65	67.5	8.57
1.0	1.66	8.44	64.0	8.97
1.2	1.56	8.30	55.7	7.21
1.4	1.55	8.02	59.1	7.35
1.6	1.51	7.51	59.0	6.69

Table S11. Tandem device performance using excitonic absorption peak at 1038 nm PbS QDs as subcell with different PbS film thickness.

Film thickness(nm)	V_{oc} (V)	J_{sc} (mA/cm ²)	FF (%)	PCE (%)
72	1.55	8.92	69.9	9.66
90	1.55	9.13	72.2	10.22
108	1.55	7.72	72.0	8.62
126	1.57	7.51	75.2	8.87
144	1.55	7.38	77.0	8.81

Table S12. Tandem device performance using excitonic absorption peak at 1254 nm PbS QDs as subcell with different PbS film thickness.

Film thickness(nm)	V_{oc} (V)	J_{sc} (mA/cm ²)	FF (%)	PCE (%)
40	1.46	8.00	61.4	7.17
60	1.51	9.47	63.8	9.12
80	1.48	9.39	71.3	9.91
100	1.53	8.73	77.1	10.30
120	1.46	8.03	76.6	8.98

Table S13. Photovoltaic parameters of tandem solar cells and perovskite solar cells with different scan directions.

Device	Direction	V_{oc} (V)	J_{sc} (mA/cm ²)	FF (%)	PCE (%)
Perovskite	Forward	1.11	17.75	68.0	13.40

	Reverse	1.11	17.69	59.6	11.70
PbS	Forward	0.56	12.21	67.0	4.58
	Reverse	0.57	12.25	65.7	4.59
Tandem	Forward	1.66	9.03	65.0	9.74
	Reverse	1.68	9.05	64.0	9.73

Table S14. Photovoltaic parameters of tandem solar cells and subcells with different UV radiation time.

Device	Time (h)	V_{oc} (V)	J_{sc} (mA/cm ²)	FF (%)	PCE (%)
Perovskite	0	1.04	17.13	80.1	14.27
	2.5	1.05	16.58	74.0	12.88
PbS	0	0.57	12.37	67.3	4.75
	2.5	0.57	12.73	68.5	4.97
Tandem	0	1.66	8.98	68.3	10.18
	2.5	1.66	8.94	67.6	10.03

References

- [1] Y. Wang, K. Lu, L. Han, Z. Liu, G. Shi, H. Fang, S. Chen, T. Wu, F. Yang, M. Gu, S. Zhou, X. Ling, X. Tang, J. Zheng, M. A. Loi, W. Ma, *Adv. Mater.* **2018**, *30*, 1704871.
- [2] W. J. Beek, M. M. Wienk, M. Kemerink, X. Yang, R. A. Janssen, *J. Phys. Chem. B* **2005**, *109*, 9505-9516.